ФИЗИКО-ХИМИЧЕСКОЕ ИЗУЧЕНИЕ КАОЛИНА МЕСТОРОЖДЕНИЯ ЖУРАВЛИНЫЙ ЛОГ. ЧАСТЬ 1

Н.В. Филатова, Н.Ф. Косенко, О.П. Денисова, К.С. Садкова

Наталья Владимировна Филатова (ORCID 0000-0001-7552-3496)*, Надежда Федоровна Косенко (ORCID 0000-0001-8806-7530), Ольга Павловна Денисова, Ксения Сергеевна Садкова

Ивановский государственный химико-технологический университет, кафедра технологии керамики и наноматериалов, пр. Шереметевский, 7, Иваново, Российская Федерация, 153000
E-mail: zyanata@mail.ru *, nfkosenko@gmail.com, denisova@mail.ru, sadkovaks@mail.ru

Значительная часть каолина, используемого в России, импортируется из Украины. Существует неотложная необходимость в импортозамещении, тем более что в России имеются соответствующие залежи алюмосиликатного сырья. Крупнейшим (более 60 млн т подтвержденных запасов первичного каолина) является месторождение чистых каолинов Журавлиный Лог (Челябинская область, Россия). В работе выполнен химический и фазовый анализ обогащенного концентрированного каолина данного месторождения. Соотношение SiO_2/Al_2O_3 в данном сырьевом материале составило 1,30. Содержание свободного оксида кварца – до 4,4%. Оксид кальция и слюда не обнаружены. Порошок каолина является тонкодисперсным (основная часть до 2 мкм) сырьевым материалом. В работе изучено термическое поведение обогащенного концентрированного каолина данного месторождения методами комплексного термического, рентгенофазового анализа и ИК-спектроскопии с преобразованием Фурье. Показано, что дегидроксилирование природного обогащенного каолина протекает при температуре примерно 500 °C, а при 910 °C метакаолинит превращается, предположительно, в кремниевую шпинель. Отсутствие пика около 250–300 °C указывает на отсутствие свободного гиббсита $Al(OH)_3$ или гётита FeOOH в обогащенном продукте. По величинам рефлексов в диапазоне 2θ 20–22° оценен индекс Хинкли (HI) как показатель порядка структуры: HI = 1,76, что указывает на высокую степень упорядоченности обогащенного каолина. После термической обработки при 400 °C индекс Хинкли снизился до 1,69. Размер кристаллитов вдоль оси с составил 61,5 нм. Муллит представлял собой основную фазу при 1200 °C.

Ключевые слова: каолин, каолинит, Журавлиный Лог, глинистые минералы, метакаолин, муллит, фазовые превращения, импортозамещение

THE PHYSICOCHEMICAL INVESTIGATION OF THE ZHURAVLINY LOG KAOLIN. PART 1

N.V. Filatova, N.F. Kosenko, O.P. Denisova, K.S. Sadkova

Natalya V. Filatova (ORCID 0000-0001-7552-3496)*, Nadezhda F. Kosenko (ORCID 0000-0001-8806-7530), Olga P. Denisova, Ksenia S. Sadkova

Department of Technology of Ceramics and Nanomaterials, Ivanovo State University of Chemistry and Technology, Sheremetevskiy ave., 7, Ivanovo, 153000, Russia
E-mail: zyanata@mail.ru *, nfkosenko@gmail.com, denisova@mail.ru, sadkovaks@mail.ru

The considerable portion of kaolin used in Russia was imported from Ukraine. There is urgent necessity to assume the measures for the import substitution in consideration of the presence of suitable deposits. The Zhuravliny Log kaolin deposit (Chelyabinsky district, Russia) is the largest one (more than sixty million tons of assured resources of the primary kaolin) in Russia. The chemical and phase composition of the concentrated kaolin was determined. The SiO_2/Al_2O_3 ratio made 1.30. The free quartz quantity was equal to 4.4%. CaO and mica were not revealed. Kaolin powders were fine-dispersed (mainly up to 2 μm). In his paper, the thermal behavior of this kaolin was

studied by the complex thermal analysis, X-ray diffractometry, and Fourier transform infrared spectroscopy. It was shown that the dehydroxylation occurred at appr. 500 °C. Further, at 910 °C metakaolinite probably turned into silica spinel. The absence of a peak at appr. 250–300 °C implies the absence of the free gibbsite Al(OH)$_3$ or goethite FeOOH. By size of reflexes in the range of 2θ 20–22° it was estimated the Hinckley index (HI) as the structure order indicator: HI made 1.76 that indicated rather high degree of order. After a heat treatment at 400 °C index reduced to 1.69. Crystallite size along the c-axis amounted 61.5 nm. Mullite was the main phase at 1200 °C.

Key words: kaolin, kaolinite, Zhuravliny Log, clay minerals, metakaolin, mullite, phase transformation, import substitution
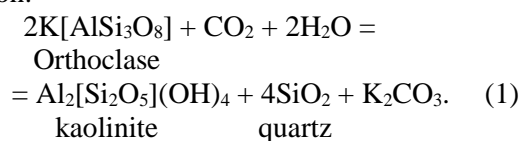
INTRODUCTION

Clay minerals are used since ancient times to make potteries and bricks. Kaolin is the purest clay rock. It is caused by its genesis from big massifs of feldspars. The main impurity is quartz as follows from the equation:

$$2K[AlSi_3O_8] + CO_2 + 2H_2O =$$
$$\text{Orthoclase}$$
$$= Al_2[Si_2O_5](OH)_4 + 4SiO_2 + K_2CO_3. \quad (1)$$
$$\text{kaolinite} \qquad \text{quartz}$$

The main rock component is kaolinite with the minimal formula $Al_2[Si_2O_5](OH)_4$, or $Al_2O_3 \cdot 2SiO_2 \cdot 2H_2O$. The considerable quantity of quartz is usually removed by means of a kaolin concentrating. Kaolinite is one of the oldest raw materials used in ceramic industry including new kinds of ceramics [1-6]. It has a wide variety of applications, particularly in the porcelain industry, ceramic tiles, sanitary wares, refractories, as a filling agent in paper, plastics, rubber, cosmetics [7, 8], as a zeolite [9, 10] and proppant precursor [11], an important geopolymer component [12-15], a pollutant sorbent [16-18], and even as a drought stress reducing agent [19], etc.

Kaolin has a global market with an estimated value of 5.43 Bn USD in 2020 and is expected to reach 8.23 Bn by 2027, at a compound annual growth rate (CAGR) of 6.5% during a forecast period. The demand for kaolin and metakaolin raised at 34, 839.9 kilo tons and 273.85 kilo tons respectively [20]. The world use of kaolin and metakaolin by application in 2016 is shown in Fig. 1 [21]. The market size is expected to grow continuously due to the increasing demand of ceramic and other products.
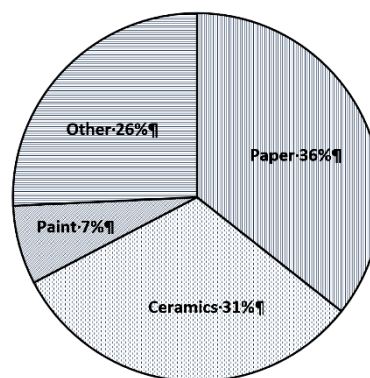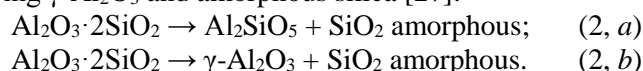

Fig. 1. Share of kaolin markets in 2016 [21]
Рис. 1. Доли рынка каолина в 2016 г. [21]

Advanced applications require a deep knowledge of the *structure – property – behavior* relationship for kaolin. The thermal behavior is of particularly interest in the ceramic production [15, 22-28]. To accelerate the product sintering, it is necessary to understand the kaolin transformations in a wide temperature range. There are the continuous loss of interlayer water (dehydration) and the discontinuous loss of structural water (dehydroxylation). Being heated to above 450-550 °C, kaolin converts irreversibly into the dehydrated metastable form, which is metakaolin (MK). When $T \sim 950$ °C, MK is transformed to a spinel structure or a Si-containing γ-Al_2O_3 and amorphous silica [27]:

$$Al_2O_3 \cdot 2SiO_2 \rightarrow Al_2SiO_5 + SiO_2 \text{ amorphous}; \quad (2, a)$$
$$Al_2O_3 \cdot 2SiO_2 \rightarrow \gamma\text{-}Al_2O_3 + SiO_2 \text{ amorphous}. \quad (2, b)$$

This problem is still under debate. Formed phases persist until at least 1100 °C turning further into mullite [15, 22-28].

The difficulty of this path investigation relates to variety of chemical composition, different particle

sizes, their distribution, etc. It is by-turn bonded to a concrete kaolin deposit. The considerable portion of kaolin used in Russia was imported from Ukraine. There is urgent necessity to assume the measures for the import substitution as it is doing in other countries [22, 29]. The Zhuravliny Log kaolin deposit is the largest one in Russia since 1992 [30-32]. It is situated in the Chelyabinsky district, near the Plast town. This deposit contains more than sixty million tons of assured resources of the primary kaolin [30]. It is suitable to produce ceramics, electro ceramics, refractories, building materials, etc. The kaolin use is strongly dependent on its structure, composition, and physicochemical properties. The aim of this research is to receive distinctive characteristics of the Zhuravliny Log kaolin and analyze them using the complex thermal analysis (thermogravimetry, TG, and differential scanning calorimetry, DSC), X-ray diffraction (XRD), and Fourier transform infrared spectroscopy (FTIR).

MATERIALS AND EXPERIMENTS

The mineral composition of a raw kaolin of the Zhuravliny Log deposit (Chelyabinsky region, Russia) has 30-70% wt. of kaolinite, 30-50% wt. of quartz, 1-18% wt. of kalium feldspar, 3-9% wt. of mica [31]. Kaolin can contain secondary components such as iron and aluminum hydroxides, quartz, feldspars, pyrite, carbonates, etc. So, kaolin must be concentrated by means of the impurity separation. Its wet concentrating with the following drying allowed to get a rather pure product which was crushed and homogenized. During storing the powder acquired the homogeneity of moisture. Its chemical composition is given in Table.

Table
The chemical composition of the concentrated Zhuravliny Log kaolin (% wt.)
Таблица. **Химический состав обогащенного каолина месторождения Журавлиный Лог (масс. %)**

SiO$_2$	Al$_2$O$_3$	TiO$_2$	Na$_2$O	CaO	MgO	K$_2$O	Fe$_2$O$_3$	LOI*
47.8	36.9	0.3	0.1	–	0.1	0.4	0.6	13.8

Note: * LOI denotes the loss on ignition at 1000 °C
Примечание: * LOI обозначает потери при прокаливании при 1000 ºC

The SiO$_2$/Al$_2$O$_3$ ratio made 1.30. The free quartz quantity was equal to 4.4%. CaO was not revealed, that implied the CaCO$_3$ absence. Kaolin powders were fine-dispersed (Fig. 2).

The kaolin size distribution was measured by a laser diffraction technique (Analisette 22 Compact) in an ethanol suspension. The chemical composition of kaolin was conducted by the disperse X-ray fluorescence (СПЕКТРОСКАН МАКС-GVM).
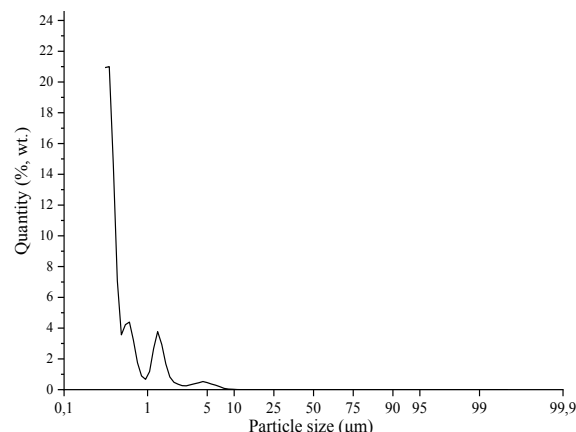

Fig. 2. Dispersion analysis of concentrated kaolin
Рис. 2. Дисперсионный анализ обогащенного каолина

Differential thermal analysis (DTA/DSC) and thermogravimetry (TGA) were recorded using NETZSCH STA 449F5 Jupiter with on-line mass-spectrometry (MS) QMS 403 Aeolos Quadro. In these tests, samples were heated up to 950 °C at a rate of 5 °C/min under an atmosphere of flowing air (50 mL/min) with α-alumina as reference substance.

XRD-patterns were obtained using a diffractometer DRON-6 with a copper target (λ = 0.1542 nm), a graphite diffracted beam monochromator, and a working voltage and current of 40 kV and 100 mA, respectively. Minerals were identified from the position of peaks and their intensities by comparison with JCPDS and ICCD database cards: Nos 14-0164 (kaolinite), 89-3433 (quartz), 82-0512 (cristobalite), 84-1205 (mullite).

FTIR absorption spectra of samples in KBr pellets were recorded on Avatar 360-FT-IR spectrometer ("Nicolet").

RESULTS

Thermal analysis is a powerful tool to understand the clay behavior under heating giving a precious information on the particularities of kaolin dehydroxylation and phase formation. Figure 3 shows the TGA and DSC curves from the room temperature up to 950 °C. Endothermic peaks on the DSC curve at low temperatures (below 110 °C) were attributed to the removal of absorbed water, including that between layers. The absence of a peak at appr. 250-300 °C implied the absence of the free gibbsite Al(OH)$_3$ or goethite FeOOH. Up to appr. 400 °C, kaolin had a small amount of the weight loss (no more than 2%). The DSC curve (Fig. 3) showed a strong endothermic peak at 500 °C, which resulted from the kaolinite dehydroxylation to the metastable metakaolinite according to the following reaction:

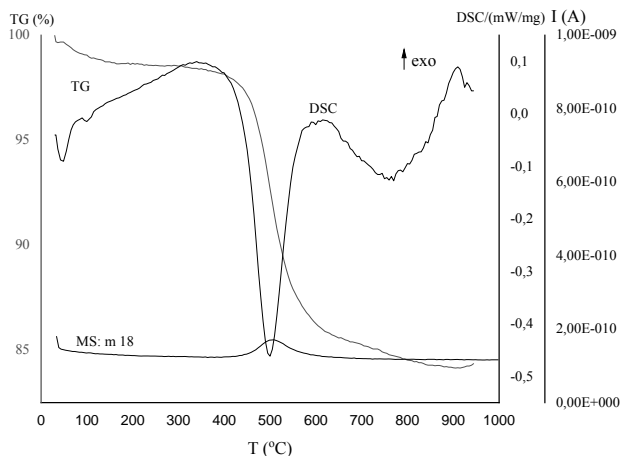$$Al_2[Si_2O_5](OH)_4 \rightarrow Al_2Si_2O_7 + 2H_2O. \quad (3)$$
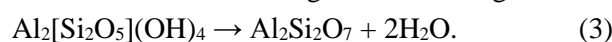
Fig. 3. TG-DSC curves of a concentrated kaolin
Рис. 3. Кривые ТГ и ДСК для обогащенного каолина

An endo peak in the range from 450 °C to 600 °C was typical for most kaolins. Exact temperature interval depends on the crystallinity and particle sizes.

The maximum location of the endothermal peak and water removal agreed as it was shown by MS-spectrometry (Fig. 3).
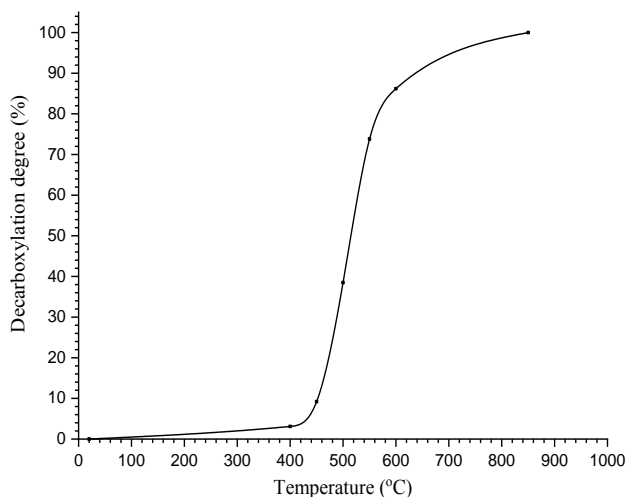

Fig. 4. Dehydroxylation degree of a heat-treated kaolin at different temperatures
Рис. 4. Степень дегидроксилирования термически обработанного каолина при различных температурах

The kaolinite dehydroxylation might result in the disturbance of the $Al(O,OH)_6$ octahedral sheet by easily removed outer hydroxyls but did not have much effect on the SiO_4 tetrahedral sheet due to the more stable inner OH-groups [27]. This process was associated with a weight loss of appr. 13%. The total mass loss related to the liberation of absorbed water and hydroxyl groups from the lattice structure of kaolinite and was appr. 15.6% from room temperature to 950 °C. A degree of a heat-treated kaolin decarboxylation as a func-

tion of temperature is shown in Fig. 4. The endothermic peak at 573 °C as a result $\alpha \leftrightarrow \beta$-inversion was absent. The quartz conversion was masked by the big and broad dehydroxylation peak within the same interval (400-600 °C). The exothermic peak at 910 °C which was not accompanied by the weight loss might indicate the metakaolin $\rightarrow$ spinel transition (reaction 2, a).
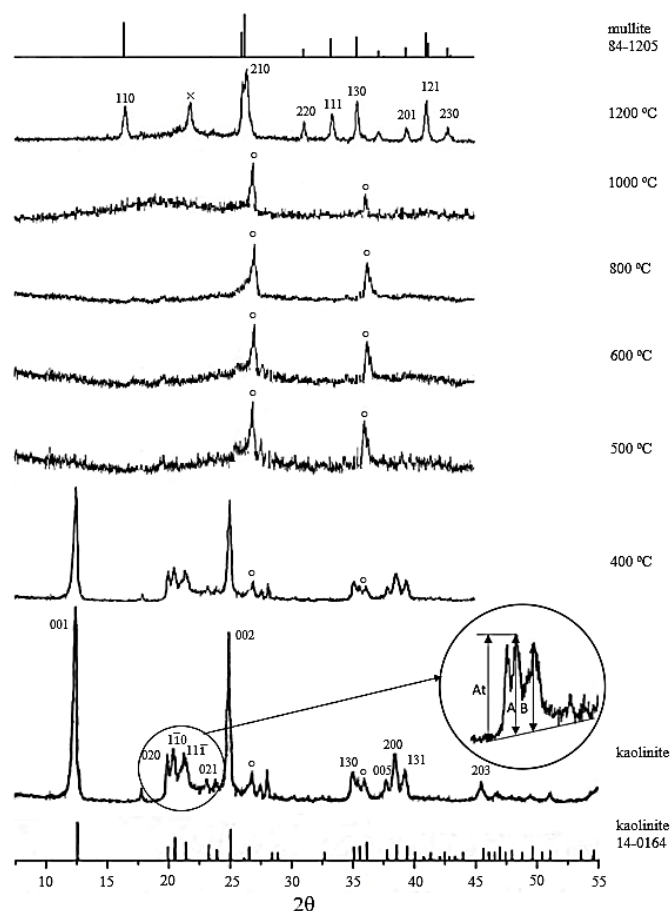
XRD patterns of kaolin samples are shown in Fig. 5.

Fig. 5. Concentrated kaolin diffractograms. Signs: o – quartz, x – cristobalite. Other peaks belong to kaolinite
Рис. 5. Дифрактограммы обогащенного каолина. Обозначения: o – кварц; x – кристобалит. Остальные пики относятся к каолиниту

First, kaolinite was indicated by its characteristic reflection peaks at 0.714 nm (001) and 0.356 nm (002). Other diffraction peaks could be also assigned to kaolinite and to a small amount of quartz. The peaks corresponding to quartz had a low intensity that indicated a low amount of free silica in studied material. No mica was observed.

Very sharp and narrow reflections lines of kaolinite (001 and 002) might denote the high degree of crystallinity. The Hinckley index (HI) [23] may esti-

mate this factor. HI is one of the most widely used indices. As illustrated in Fig. 4 (the round inset), it is the ratio of the height above background of the $1\bar{1}0$ (A) and $11\bar{1}$ (B) peaks above the band of overlapping peaks occurring between 20–22° 2θ compared to the total height of the $1\bar{1}0$ above background (At):

$$HI = (A+B)\ /At. \qquad (4)$$

Normal values range from <0.5 (disordered) to 1.5 upwards (ordered). For concentrated Zhuravliny Log kaolin, HI = 1.76 that indicates low-defect kaolin. After heating at 400 °C, kaolin HI reduced to 1.69.

The average flake thickness of kaolin along the c-axis D was estimated according to the Debye-Scherrer equation:

$$D = K\lambda\ /\ \beta\cos\theta, \qquad (5)$$

where K is the Scherrer constant that depends on the shape and size distribution; λ is the X-ray wavelength; β and θ are full-width-at-half-maximum (FWHM) of an observed peak and diffraction angle, respectively.

As FWHM of (001) peak was equal to 0.260°, crystallite size amounted 61.5 nm.

After a kaolin burning at 500 °C, sharp kaolinite reflexes (001 and 002) and characteristic peaks between 20 and 23 2θ disappeared with the kaolinite structure completely lost. Metakaolinite is a result of hydroxyl groups removing above 400 °C (Fig. 4) and is described as X-ray amorphous, but it demonstrates two-dimensional regularity in the kaolin layers, which are stacked so that the three-dimensional periodicity is absent [28]. So, it could not be identified by XRD. The characteristic diffraction peaks of quartz could always be seen during the thermal treatment at different temperatures (up to 1000 °C). Thermodynamically stable mullite phase was dominant at 1200 °C as all characteristic diffraction peaks were observed. At this temperature, the amorphous SiO_2 changed to cristobalite.

Unfortunately, the large part of diffractograms for burned kaolin (500-1000 °C) indicated the amorphous character of substances excepting the free quartz. So, for the more detailed description IR-spectral analysis was conducted. FTIR spectra of a raw kaolin and its products burned at 500, 600, 700, 800, 900, 1000, and 1200 °C are shown in Fig. 6, a-h, respectively. First, one can suggest that the broadened band at 3448-3428 cm⁻¹ is not linked to the kaolinite structure. It relates to valent vibrations of OH-groups of absorbed water which is almost always present in kaolins. (Proper deformation vibration at 1630 cm⁻¹ was in scrap.).

Spectra of a raw kaolin and a product obtained at 500 °C were principally differed from the others (Fig. 6, a, b). They had an absorption band multiplet at 3700-3620 cm⁻¹ which described stretching (valent) vibrations of the inner-surface hydroxyl groups in the interlayer (3695, 3670, 3650 cm⁻¹) and the same vibrations of the inner hydroxyl groups of Al^{VI}-O octahedrons (3620 cm⁻¹) [15, 25]. A raw kaolin being well-ordered (HI = 1.76), it was observed separate bands in the first group (3694-3696 cm⁻¹, marked kinks near 3670 and 3650 cm⁻¹).

The characteristic bending peaks of the four analogous Al^{VI}–OH bonds were located at 937 (shoulder), 915, 794-798, and 755 cm⁻¹. Some reduction of the characteristic peak intensity of a burned kaolin indicated its partial dehydroxylation at 500 °C. The absorptions centered at appr. 1100, 690 and 470 cm⁻¹ were contributed to internal vibration bands of T-O-T (where T denotes Al or Si): stretching, bending, and rocking, respectively [25]. In the first place, bands at 1100-1000 cm⁻¹ might be attribute to Si–O (appr. 1100 cm⁻¹) and Si–O–Si (1033, 1011 cm⁻¹) valent vibrations. Compared with a raw kaolin, their location under heating was unchanged, while the peak intensity and its form were changed. Bands being primarily resolved (Fig. 6, a, b), were gradually blended (Fig. 6, c–h). Si–O–Si vibrations at 461-476 cm⁻¹ existed in the all range of temperature that testified the invariance of silica-oxygen coordination tetrahedrons (Fig. 6, a–h).

The bands at 540 and 432-441 cm⁻¹ (Fig. 6, a, b) might belong to the internal deformation vibration band of Si-O-Al^{VI}. When the burning temperature increased to 600 °C, the vibration peaks of O–H (3700-3620 cm⁻¹) and Al^{VI}–OH bonds (937, 915, 794, and 755 cm⁻¹) of the samples completely disappeared (Fig. 6, c), indicating that the dehydroxylation of kaolinite was over. After burning at 600 °C, the Al–O group of the products was changed; and the Al^{IV}–O bond of AlO_4 appeared at the 803-811 cm⁻¹ [25]. When rising to 900 °C, the Al–O groups of the burning products no longer changed. The Si–O–Al peak changed to a higher wave number at 563 cm⁻¹.

The set of bands at 1160 (shoulder), 899, 736, and 562 might be attributed to mullite [33] that confirmed its monophase presence at 1200 °C.

Further, it will be discussed data of nuclear magnetic resonance, dilatometry, zeta-potential for a concentrated Zhuravliny Log kaolin.

CONCLUSION

Transformations of a concentrated Zhuravliny Log kaolin were described using the complex thermal method, X-ray diffractometry, and infrared spectroscopy. It was shown that the main dehydroxylation run at 500 °C. Further, the formed metakaolinite probably turned into a silica spinel at 910 °C. Mullite was the single phase at 1200 °C. It was estimated the Hinckley index (HI) as the structure order indicator: HI made 1.76 that indicated high degree of order. Crystallite size along the c-axis amounted 61.5 nm.
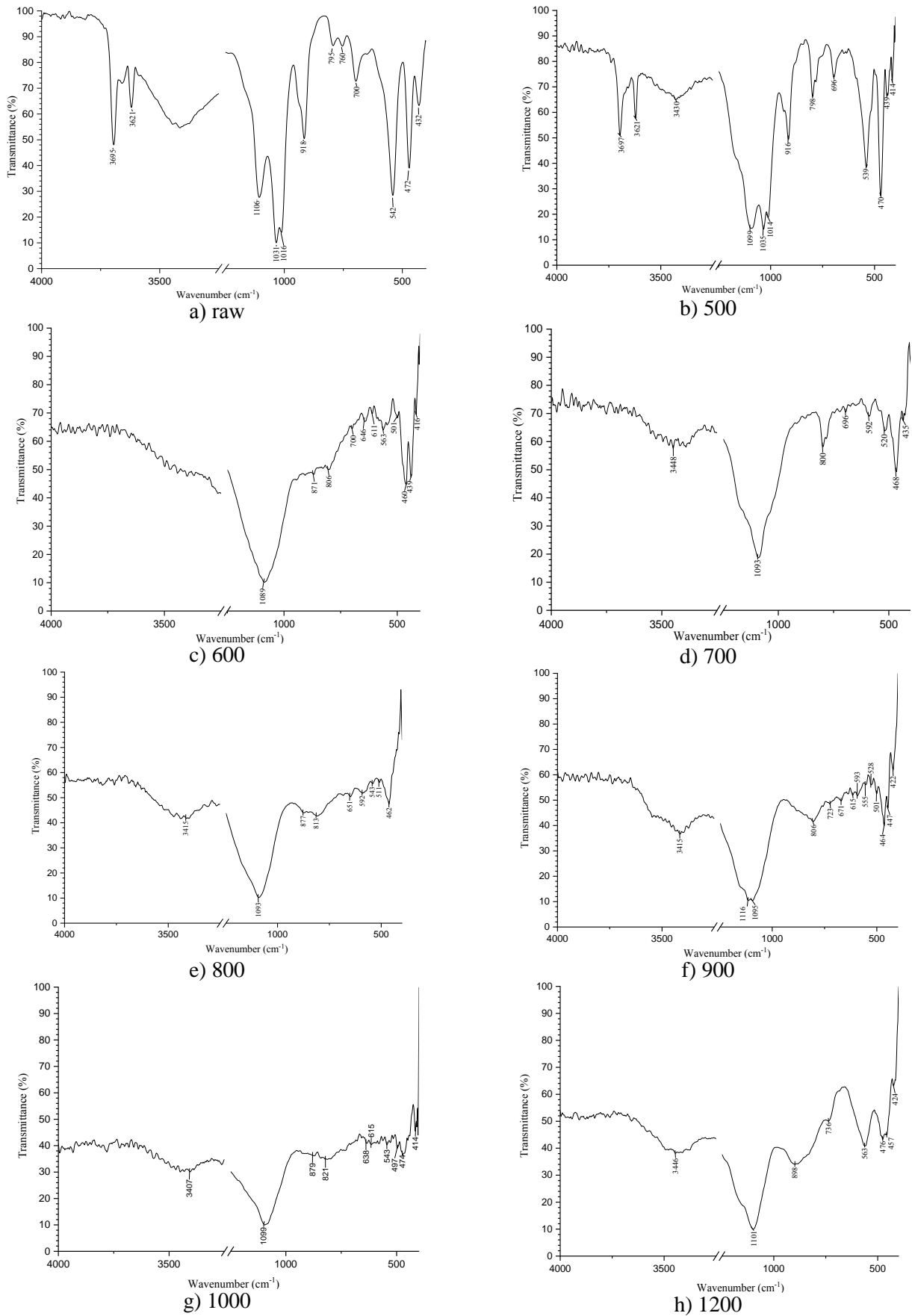
Fig. 6. FTIR-spectra of concentrated kaolin
Рис. 6. FTIR-спектры обогащенного каолина

90

Изв. вузов. Химия и хим. технология. 2022. Т. 65. Вып. 8

ЛИТЕРАТУРА

1. **Fierascu I., Baroi A.M., Brazdis R.I., Fistos T., Nicolae C.A., Raditoiu V., Inel I.C., Sava V., Fierascu R.C.** Archaeometrical Characterization of Romanian Late Bronze Age Ceramic Fragments. *Front. Mater.* 2021. V. 8. Art. 630137. DOI: 10.3389/fmats.2021.630137.

2. **Murray H.H.** Applied clay mineralogy. Occurrences, Processing and Application of Kaolins, Bentonites, Palygorskite, Sepiolite, and Common Clays. Elsevier. 2007. 189 p. DOI: 10.1016/S1572-4352(06)02008-3.

3. **Boudchicha M.R., Rubio F., Achour S.** Synthesis of glass ceramics from kaolin and dolomite mixture. *Int. J. Miner., Metall., Mater.* 2017. V. 24. P. 194–201. DOI: 10.1007/s12613-017-1395-4.

4. **Usman J., Othman M.H.D., Ismail A.F., Rahman M.A., Jaafar J., Abdullahi T.** Comparative study of Malaysian and Nigerian kaolin-based ceramic hollow fiber membranes for filtration application. *Malaysian J. Fund. Appl. Sci.* 2020. V. 16. N 2. P. 182-185. DOI: 10.11113/mjfas.v16n2.1484.

5. **Mocciaro A.,·Conconi M.S., Rendtorff N.M., Scian A.N.** Ceramic properties of kaolinitic clay with monoaluminum phosphate ($Al(H_2PO_4)_3$) addition. *J. Therm. Anal. Calorim.* 2021. V. 144. N 4. P. 1083–1093. DOI: 10.1007/s10973-020-10488-2.

6. **Yang X., Yang W., Hu J.** Preparation of Low-Dielectric-Constant Kaolin Clay Ceramics by Chemical Cleaning Method. *Front. Mater.* 2021. V. 8. Art. 692759. DOI: 10.3389/fmats.2021.692759.

7. **Ahmed N.M.** Comparative study on the role of kaolin, calcined kaolin and chemically treated kaolin in alkyd-based paints for protection of steel. *Pigment Resin Technol.* 2013. V. 42. N 1. P. 3–14. DOI: 10.1108/03699421311288715.

8. **Frías M., Rodríguez O., De Rojas M.S.** Paper sludge, an environmentally sound alternative source of MK-based cementitious materials. A review. *Construct. Build. Mater.* 2015. V. 74. P. 37–48. DOI: 10.1016/j.conbuildmat.2014.10.007.

9. **Гордина Н.Е.** Механохимическая активация как способ интенсификации процессов синтеза низкомодульных цеолитов. *Изв. вузов. Химия и хим. технология.* 2018. Т. 61. Вып. 7. С. 4-22. DOI: 10.6060/ivkkt.20186107.5687.

10. **Гордина Н.Е., Прокофьев В.Ю., Борисова Т.Н., Елизарова А.М.** Синтез гранулированных низкомодульных цеолитов из метакаолина с использо-ванием механохимической активации и ультразвуковой обработки. *Изв. вузов. Химия и хим. технология.* 2019. Т. 62. Вып. 7. С. 99-106. DOI: 10.6060/ivkkt201962fp.5725.

11. **Mocciaro A., Lombardi M.B., Scian A.N.** Effect of raw material milling on ceramic proppants properties. *Appl. Clay Sci.* 2018. V. 153. P. 90-94. DOI: 10.1016/j.clay.2017.12.009.

REFERENCES

1. **Fierascu I., Baroi A.M., Brazdis R.I., Fistos T., Nicolae C.A., Raditoiu V., Inel I.C., Sava V., Fierascu R.C.** Archaeometrical Characterization of Romanian Late Bronze Age Ceramic Fragments. *Front. Mater.* 2021. V. 8. Art. 630137. DOI: 10.3389/fmats.2021.630137.

2. **Murray H.H.** Applied clay mineralogy. Occurrences, Processing and Application of Kaolins, Bentonites, Palygorskite, Sepiolite, and Common Clays. Elsevier. 2007. 189 p. DOI: 10.1016/S1572-4352(06)02008-3.

3. **Boudchicha M.R., Rubio F., Achour S.** Synthesis of glass ceramics from kaolin and dolomite mixture. *Int. J. Miner., Metall., Mater.* 2017. V. 24. P. 194–201. DOI: 10.1007/s12613-017-1395-4.

4. **Usman J., Othman M.H.D., Ismail A.F., Rahman M.A., Jaafar J., Abdullahi T.** Comparative study of Malaysian and Nigerian kaolin-based ceramic hollow fiber membranes for filtration application. *Malaysian J. Fund. Appl. Sci.* 2020. V. 16. N 2. P. 182-185. DOI: 10.11113/mjfas.v16n2.1484.

5. **Mocciaro A.,·Conconi M.S., Rendtorff N.M., Scian A.N.** Ceramic properties of kaolinitic clay with monoaluminum phosphate ($Al(H_2PO_4)_3$) addition. *J. Therm. Anal. Calorim.* 2021. V. 144. N 4. P. 1083–1093. DOI: 10.1007/s10973-020-10488-2.

6. **Yang X., Yang W., Hu J.** Preparation of Low-Dielectric-Constant Kaolin Clay Ceramics by Chemical Cleaning Method. *Front. Mater.* 2021. V. 8. Art. 692759. DOI: 10.3389/fmats.2021.692759.

7. **Ahmed N.M.** Comparative study on the role of kaolin, calcined kaolin and chemically treated kaolin in alkyd-based paints for protection of steel. *Pigment Resin Technol.* 2013. V. 42. N 1. P. 3–14. DOI: 10.1108/03699421311288715.

8. **Frías M., Rodríguez O., De Rojas M.S.** Paper sludge, an environmentally sound alternative source of MK-based cementitious materials. A review. *Construct. Build. Mater.* 2015. V. 74. P. 37–48. DOI: 10.1016/j.conbuildmat.2014.10.007.

9. **Gordina N.E.** Mechanochemical activation as method of intensifying synthesis processes of low-modulus zeolites. *ChemChemTech [Izv. Vyssh. Uchebn. Zaved. Khim. Khim. Tekhnol.].* 2018. V. 61. N 7. P. 4-22 (in Russian). DOI: 10.6060/ivkkt.20186107.5687.

10. **Gordina N.E., Prokof`ev V.Yu., Borisova T.N., Elizarova A.M.** Synthesis of granular low-modulus zeolites from metakaolin using mechanochemical activation and ultrasonic treatment. *ChemChemTech [Izv. Vyssh. Uchebn. Zaved. Khim. Khim. Tekhnol.].* 2019. V. 62. N 7. P. 99-106 (in Russian). DOI: 10.6060/ivkkt201962fp.5725.

11. **Mocciaro A., Lombardi M.B., Scian A.N.** Effect of raw material milling on ceramic proppants properties. *Appl. Clay Sci.* 2018. V. 153. P. 90-94. DOI: 10.1016/j.clay.2017.12.009.

12. **Bewa C.N., Tchakoute H.K., Banenzoue C., Cakanou L., Mbakop T.T., Kamseu E., Ruscher C.H.** Acid-based geopolymers using waste fired brick and different metakaolins as raw materials. *Appl. Clay Sci.* 2020. V. 198. 105813. DOI: 10.1016/j.clay.2020.105813Get.

13. **Jindal B.B., Alomayri T., Hasan A., Kaze C.R.** Geopolymer concrete with metakaolin for sustainability: a comprehensive review on raw material's properties, synthesis, performance, and potential application. *Environ. Sci. Pollut. Res.* 2022. Jan 9. DOI: 10.1007/s11356-021-17849-w.

14. **Liu X., Jiang J., Zhang H., Li M., Wu Y., Guo L., Wang W., Duan P., Zhang W., Zhang Z.** Thermal stability and microstructure of metakaolin-based geopolymer blended with rice husk ash. *Appl. Clay Sci.* 2020. V. 196. 105769. DOI: 10.1016/j.clay.2020.105769.

15. **Jia D., He P., Wang M., Yan Sh.** Geopolymer and Geopolymer Matrix Composites. Springer Nature Singapore Pte Ltd. 2020. 310 p. DOI: 10.1007/978-981-15-9536-3.

16. **Khairy M., Ayoub H.A., Rashwan F.A., Abdel-Hafez H.F.** Chemical modification of commercial kaolin for mitigation of organic pollutants in environment via adsorption and generation of inorganic pesticides. *Appl. Clay Sci.* 2018. V. 153. P. 124–133. DOI: 10.1016/j.clay.2017.12.014.

17. **Mustapha S., Tijani J.O., Ndamitso M.M., Abdulkareem S.A., Shuaib D.T., Mohammed A.K., Sumaila A.** The role of kaolin and kaolin/ZnO nanoadsorbents in adsorption studies for tannery wastewater treatment. *Sci. Rep.* 2020. V. 10. P. 13068. DOI: 10.1038/s41598-020-69808-z.

18. **Zhang Q., Yan Z., Ouyang J., Zhang Y., Yang H., Chen D.** Chemically modified kaolinite nanolayers for the removal of organic pollutants. *Appl. Clay Sci.* 2018. V. 157. P. 283–290. DOI: 10.1016/j.clay.2018.03.009.

19. **Faghih S., Zamani Z., Fatahi R., Omidi M.** Influence of kaolin application on most important fruit and leaf characteristics of two apple cultivars under sustained deficit irrigation. *Biolog. Res.* 2021. V. 54. N 1. DOI: 10.1186/s40659-020-00325-z.

20. **Kumar S.** Kaolin Market Size, Share & Trends Analysis Report by Application (Ceramics, Plastic, Pharmaceuticals & Medical, Paint & Coatings, Cosmetics, Fiber Glass, Paper, Rubber), by Region, and Segment Forecasts, 2019–2025. *Res. Market.* 2019. DOI: 10.1016/j.focat.2019.06.012.

21. **Rackstraw P.** Positive outlook for kaolin in ceramics. *Indust. Minerals.* 2019. N 609. P. 28-32.

22. **Badr M.S.H., Yuan Sh., Dong J., El-Shall H., Bermudez Y.A., Ortega D.C., Lopez-Rendon J.E., Moudgil B.M.** The Properties of Kaolin from Different Locations and Their Impact on Casting Rate. *KONA Powder Part. J.* 2020. V. 38. P. 251-259. DOI: 10.14356/kona.2021002.

23. **Cheng Y., Xing J., Bu Ch., Zhang J., Piao G., Huang Y., Xie H., Wang X.** Dehydroxylation and Structural Distortion of Kaolinite as a High-Temperature Sorbent in the Furnace. *Minerals.* 2019. V. 9. N 10. P. 587. DOI: 10.3390/min9100587.

24. **Tchanang G., Djangang Ch.N., Abi C.F., Moukouri D.L.M., Blanchart Ph.** Synthesis of reactive silica from kaolinitic clay: Effect of process parameters. *Appl. Clay Sci.* 2021. V. 207. P. 106087. DOI: 10.1016/j.clay.2021.106087.

25. **Yan K., Guo Y., Fang L., Cui L., Cheng F., Li T.** Decomposition and phase transformation mechanism of kaolinite calcined with sodium carbonate. *Appl. Clay Sci.* 2017. V. 147. P. 90–96. DOI: 10.1016/j.clay.2017.07.010.

92

Изв. вузов. Химия и хим. технология. 2022. Т. 65. Вып. 8

26. **Xu X., Lao X., Wu J., Zhang Y., Xu X., Li K.** Microstructural evolution, phase transformation, and variations in physical properties of coal series kaolin powder compact during firing. *Appl. Clay Sci.* 2015. V. 115. P. 76–86. DOI: 10.1016/j.clay.2015.07.031.

27. **Ghorbel A., Fourati M., Bouaziz J.** Microstructural evolution and phase transformation of different sintered Kaolins powder compacts. *Mater. Chem. Phys.* 2008. V. 112. N 3. P. 876–885. DOI: 10.1016/j.matchemphys.2008.06.047.

28. **Sperinck Sh., Raiteri P., Marks N., Wright K.** Dehydroxylation of Kaolinite to Metakaolin - A Molecular Dynamics Study. *J. Mater. Chem.* 2011 V. 21. N 7. P. 2118-2125. DOI: 10.1039/C0JM01748E.

29. **Шиманская А.Н., Дятлова Е.М., Попов Р.Ю.** Огнеупорное глинистое сырье Республики Беларусь для производства керамогранита. *Изв. вузов. Химия и хим. технология.* 2019. Т. 62. Вып. 12. С. 39-44. DOI: 10.6060/ivkkt.20196212.6018.

30. URL: http://kaolinzhl.ru/company/ (дата обращения: 20.02.2022).

31. **Солодкий Н.Ф., Солодкая М.Н., Шамриков А.С.** Использование каолина месторождения "Журавлиный Лог" в производстве тонкой керамики. *Огнеупоры и техн. керамика.* 2000. № 5. С. 34-35.

32. **Аргынбаев Т.М., Стафеева З.В., Белогуб Е.В.** Месторождение каолинов Журавлиный Лог – комплексное сырье для производства строительных материалов. *Строит. материалы.* 2014. № 5. С. 68-71.

33. **Li J., Lin H., Li J., Wu J.** Effects of different potassium salts on the formation of mullite as the only crystal phase in kaolinite. *J. Eur. Ceram. Soc.* 2009. V. 29. N 14. P. 2929–2936. DOI: 10.1016/j.jeurceramsoc.2009.04.032.